Integral control of smart structures with collocated sensors and actuators

Sumeet S. Aphale, Andrew J. Fleming and S. O. Reza Moheimani*

Abstract— **This paper introduces a novel way of implementing simple first- and second-order feedback controllers, for vibration control in smart structures with collocated sensors and actuators. As these controllers are motivated by the simple integrator, the scheme is called Integral Resonant Control (IRC). In this approach a direct feed-though is added to a collocated system and the transfer function is modified such that it contains zeros followed by interlaced poles. This modification permits the application of the IRC scheme which results in good performance and stability margins. Problems due to unnecessarily high controller gain below the first mode are alleviated by slightly increasing the complexity from a first to a second order controller. Experiments carried out on a piezoelectric laminate cantilever beam demonstrate up to 24 dB modal amplitude reduction over the first eight modes.**

I. Introduction

The presence of noise and vibration is of great concern in many industrial, scientific and defense applications [1], [2], [3]. Smart Structures have shown potential to offer improved vibration control in applications where passive techniques are either insufficient or impractical. Active structural control involves two main tasks; selection and integration of actuators and sensors, and the control system design. This work proposes a new control methodology for smart structures with collocated piezoelectric actuators and sensors. Piezoelectric materials have emerged as the transducer of choice in the field of smart structures. Their small volume, low weight and ease of structural integration, are some of the many desirable properties exhibited by these unique materials [4], [5], [6], [7].

Designing an effective control strategy for flexible structures presents many difficulties due to inherent system properties such as variable resonance frequencies, high system order, and highly resonant dynamics. Many traditional control techniques such as LQG, H_2 and H_∞ have been researched and documented by earlier researchers [8], [9]. These techniques tend to result in control systems of high-order and poor stability margins. Thus a simple, robust and well-performing control technique is sought after.

It has proved beneficial to exploit the underlying structure of a collocated resonant mechanical system while designing controllers for damping resonant vibration modes. Greater robustness, performance, and ease of implementation relative to traditional techniques are some of their well-known benefits. The most useful characteristic of a collocated system is the interlacing of poles and zeros up the $j\omega$ axis. This results in a phase response that lies continuously between 0 and -180 degrees. This property has been successfully exploited by Positive Position Feedback (PPF) [10], a popular control design technique. PPF controllers come with many built-in benefits such as stability in the presence of uncontrolled in-bandwidth modes and quick roll off at higher frequencies which, in turn, reduces the risk of destabilizing systems with high-frequency dynamics. Their main drawback is that the PPF controllers are also equal in order to the system which they are designed to control. Furthermore, they require a model based design process (often requiring a non-linear search); and they are difficult to tune if more than one mode is to be controlled. The phase profile of collocated system is also exploited in another control technique known as Velocity feedback [11]. In theory, velocity feedback implements pure viscous damping with a phase margin of 90 degrees. Unfortunately, the high frequency gain must be attenuated to avoid noise amplification and destabilization due to unmodeled or non-collocated dynamics. Due to the two additional poles required at high frequencies, velocity feedback results in relatively low performance and poor phase margin. Resonant control has also been successfully applied to collocated resonant systems [12]. Though this technique guarantees closed-loop stability in the presence of unmodeled out-of-band modes, the high-pass nature of the controller may deem it unsuitable in certain scenarios.

The control design proposed in this work is based on augmenting the feed-through of a collocated system by adding a small portion of the actuator signal to the sensor signal. Section III will show that this procedure results in the addition of a pair of resonant system zeros at an arbitrarily chosen frequency. Choosing this frequency lower than the first mode results in a compound system with interlaced zeros then poles, rather than poles then zeros. The phase response of this system lies between 0 and +180 degrees. This property can be exploited through the use of direct integral feedback which results in a loop phase response that lies between -90 and $+90$ degrees. Direct integral strain feedback has the benefit of substantial damping augmentation while naturally rolling off at higher frequencies.

The following section states the objectives and scope of this work together with a description of the experimental apparatus. The characteristics of collocated systems, feed-though augmentation, and integral feedback design are then discussed in Section III. Experimental results demonstrating

This work was supported by the Australian Research Council's Center for Complex Dynamic Systems and Control

Authors are with School of Electrical Engineering and Computer Science, University of Newcastle, Callaghan NSW 2308, Australia (sumeet.aphale, andrew.fleming, reza.moheimani) @newcastle.edu.au

* Corresponding author

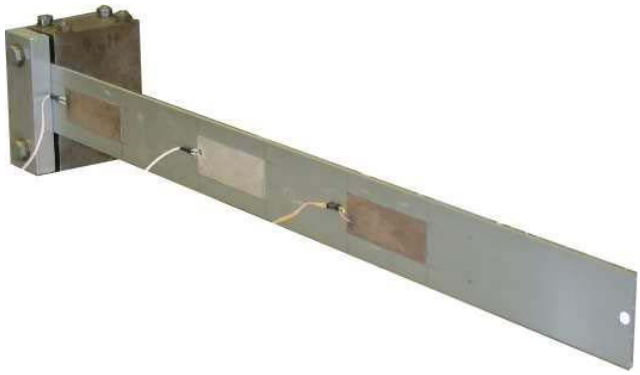

Fig. 1. Picture of the cantilever beam.

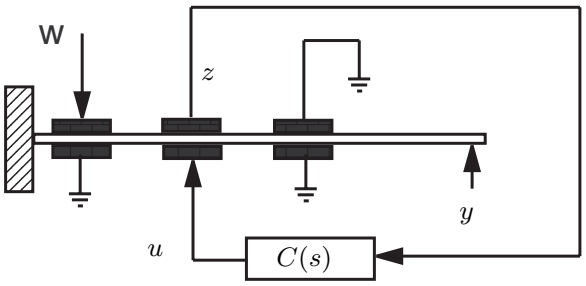

Fig. 2. Schematic diagram of the control strategy showing the inputs and outputs.

up to 24 dB reduction over eight modes are presented in Section IV followed by concluding remarks in Section V.

II. Objectives

The main objective of this work is to propose, implement and evaluate a simple and robust control technique to damp multiple low-frequency modes of a class of resonant mechanical systems that exhibit interlaced poles and zeros in their collocated transfer functions. We begin by analyzing the interesting properties of transfer functions of resonant systems with collocated sensors and actuators. This will be followed by a mathematical proof for the pole-zero interlacing phenomenon in such transfer functions. It is shown that a pair of resonant zeros can be added at an arbitrarily chosen frequency by adding a specific feed-through term to this transfer function. A parametric form of the appropriate feed-through term necessary to manipulate the pole-zero interlacing of the collocated transfer function is formulated. Furthermore, analysis of this modified transfer function shows that simple second-order controllers based on the integral controller, can be implemented to damp vibrations over multiple low-frequency resonant modes. This scheme is called the Integral Resonant Control (IRC) scheme. A cantilever beam, which is clamped at one end and free at the other end is a well-known example of a resonant mechanical system susceptible to high amplitude vibrations when disturbed. A piezoelectric laminate cantilever beam is used to experimentally verify our theoretical results.

A. Experimental setup

Figure 1 shows the piezoelectric laminate cantilever beam used in this work. This cantilever beam has three pairs (sensor-actuator) of collocated piezoelectric patches attached to it. In this work, one collocated pair is used for actuation and sensing. The second collocated pair is shorted, thus for all practical purposes, it has no effect on the open or closed loop beam dynamics. Of the third collocated pair, one patch is shorted and the other is used as an independent disturbance source. This arrangement replicates most practical disturbance sources.

The equivalent two-input two-output system of the cantilever beam is shown in Figure 2. The inputs are the control voltage applied to the collocated actuator patch (u) and the disturbance generated by the third (non-collocated) piezo-patch (w). The outputs are the collocated sensor voltage (y) and the tip displacement (z).

The frequency response functions (FRF) correspond to a particular combination of the input and the output (for example $G_{yw}(\mathrm{j}\omega) = y(\mathrm{j}\omega)/w(\mathrm{j}\omega)$ when $u = 0$). They are determined by applying a sinusoidal chirp of varying frequency (from 5-250Hz) as inputs (w and u) to the corresponding piezoelectric actuators and measuring the output signals (y and z). This frequency range (from 5-250Hz) captures the first three resonant modes of the cantilever beam. A Polytec Scanning Laser Vibrometer (PSV-300) was used to record all the needed FRFs.

III. Controller design

A model of the system is required to analyze and design a control strategy. A subspace based modeling technique [13] is used to procure an accurate model of the cantilever beam system. Figures 3 and 4 show the magnitude and phase responses of the modeled and the actual system. The model captures the dynamics of the system with high accuracy.

A. Properties of collocated transfer functions

The transfer function associated with a single collocated actuator/sensor pair displays many interesting properties [14], [15]. It is a minimum phase system where the poles and zeros of the system interlace. This ensures that the phase of a collocated transfer function will be within 0° and -180°. The system transfer function can be represented as the sum of many second order blocks and can be written as

$$G(s) = \sum_{i=1}^{M} \frac{\alpha_i}{s^2 + 2\zeta_i\omega_i s + \omega_i^2} \qquad (1)$$

where $\alpha_i > 0 \quad \forall i$ and $M \to \infty$ [16]. A very large but finite M represents the number of modes that sufficiently describe the elastic properties of the structure under excitation. In most cases, $N < M$ modes of the structure would fit in the 'bandwidth of interest' and are controlled (damped)

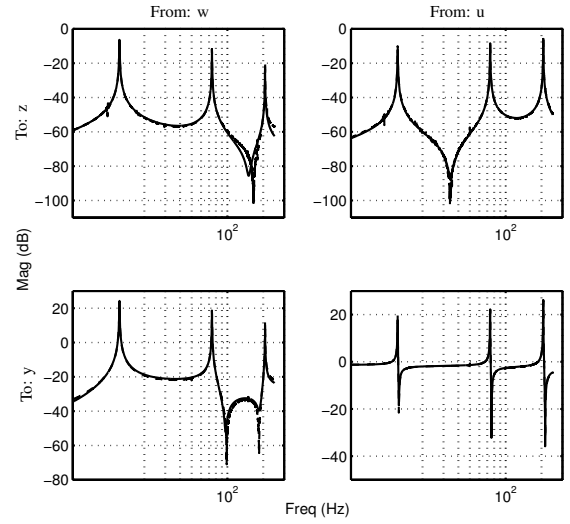

Fig. 3. Magnitude response of the measured (- -) and modeled (—) system.

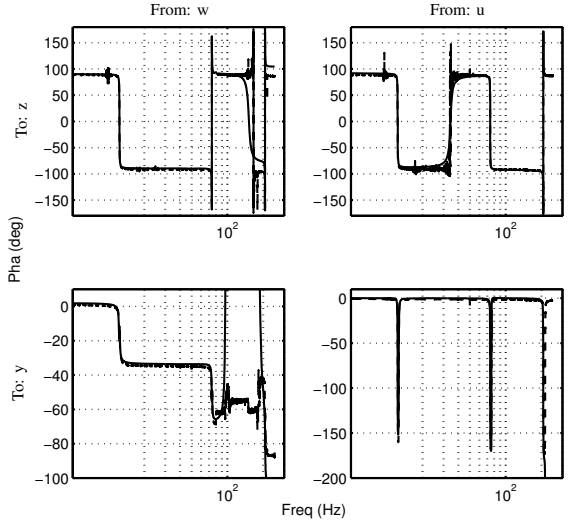

Fig. 4. Phase response of the measured (- -) and modeled (—) system.

while modes $N+1$ and above are left uncontrolled. The out-of-band (truncated) poles have a significant effect on the in-band zeros and this can potentially destabilize the closed-loop system, if left unaccounted. To guarantee that unmodeled high frequency modes do not affect the position of low frequency zeros, a feed-through term is added to the truncated model [17]. The resulting system can be written as,

$$\tilde{G}(s) = \sum_{i=1}^{N} \frac{\alpha_i}{s^2 + 2\zeta_i\omega_i s + \omega_i^2} + D \qquad (2)$$

where $D \in \mathbb{R}$. Note that the parametric model for the collocated transfer function $G_{yu}(s)$ is of the form (2). The remaining transfer functions are of the form (1), but with no positivity constraint on α_i, see Figure 3(a).

B. Feed-through and pole-zero interlacing

This section will mathematically explain the interlacing pole-zero pattern exhibited by a collocated transfer function. The effect a particular choice of feed-through (D) will have on the truncated system model will also be discussed in detail. For the sake of brevity, zero damping is assumed in the following analysis ($\zeta = 0$). However, the results can easily be extended to include systems with damping [1].

Theorem *1:* Let $G(s) = \sum_{i=1}^{N} \frac{\alpha_i}{s^2+\omega_i^2}$ such that $\alpha_i > 0$ for $i = 1, 2, 3, \cdots$ and $\omega_1 < \omega_2 < \cdots < \omega_N$. Then, between every two consecutive poles of $G(s)$ there exist a zero.

Proof: We begin with a truncated case of $G(s)$ denoted by $\hat{G}(s)$ such that,

$\hat{G}(s) = \sum_{i=1}^{3} \frac{\alpha_i}{s^2+\omega_i^2}$. Expanding, we get

$$\hat{G}(s) = \frac{\alpha_1}{s^2+\omega_1^2} + \frac{\alpha_2}{s^2+\omega_2^2} + \frac{\alpha_3}{s^2+\omega_3^2}$$

Expanding and collecting terms we get,

$$\hat{G}(s) = \frac{\alpha_1(s^2+\omega_2^2)(s^2+\omega_3^2)+\alpha_2(s^2+\omega_1^2)(s^2+\omega_3^2)+\alpha_3(s^2+\omega_1^2)(s^2+\omega_2^2)}{(s^2+\omega_1^2)(s^2+\omega_2^2)(s^2+\omega_3^2)}$$

The numerator of $\hat{G}(s)$ is a polynomial in s^2. Let this be known as $N(s^2)$. Then,

$$N(s^2)\mid_{s^2=-\omega_1^2} = \alpha_1(-\omega_1^2+\omega_2^2)(-\omega_1^2+\omega_3^2) > 0$$

as $\alpha_i > 0 \quad \forall i$ and $\omega_1 < \omega_2 < \omega_3$. Similarly,

$$N(s^2)\mid_{s^2=-\omega_2^2} = \alpha_1(-\omega_1^2+\omega_2^2)(-\omega_1^2+\omega_3^2) < 0$$

and

$$N(s^2)\mid_{s^2=-\omega_3^2} = \alpha_1(-\omega_1^2+\omega_2^2)(-\omega_1^2+\omega_3^2) > 0$$

$N(s^2)$ is a continuous function in s. The value of $N(s^2)\mid_{s^2=-\omega_1^2}$ is positive while at $N(s^2)\mid_{s^2=-\omega_2^2}$ is negative. $N(s^2)$ must therefore, be 0 for a value of s^2 somewhere between $-\omega_1^2$ and $-\omega_2^2$. Thus for $s^2 = -\omega_{z_1}^2$ such that $\omega_1 < \omega_{z_1} < \omega_2$, $N(-\omega_{z_1}^2) = 0$. Similarly, it can be shown that $N(-\omega_{z_2}^2) = 0$ where $\omega_2 < \omega_{z_2} < \omega_3$.

Using the same argument for the numerator of $G(s)$ (untruncated) it can be shown that there exist $n-1$ zeros $\omega_{z_1}, \omega_{z_2}, \cdots, \omega_{z_{n-1}}$ for $G(s) = \sum_{i=1}^{N} \frac{\alpha_i}{s^2+\omega_i^2}$ such that, $\omega_1 < \omega_{z_1} < \omega_2 < \cdots < \omega_{z_{n-1}} < \omega_N$, i.e. between every two consecutive poles lies a zero. ∎

This theorem shows that a system obtained by adding N second order terms of the form $\frac{\alpha_i}{s^2+\omega_i^2}$ has N pairs or complex conjugate (resonant) poles and $N-1$ pairs of

[1]Note that as these systems have extremely small damping coefficients (ζ), the effect of the damping term is only to shift the poles and zeros to the left half plane by a small real value.

complex conjugate (resonant) zeros such that between every two poles, there is a zero.

Theorem *2:* Let $G(s) = \sum_{i=1}^{N} \frac{\alpha_i}{s^2+\omega_i^2}$ such that $\alpha_i > 0 \quad \forall i$ and $\omega_1 < \omega_2 < \cdots < \omega_N$. If $\tilde{G}(s) = G(s) + D$ such that $D \in \mathbb{R}$ and $\tilde{G}(j\omega_z) = 0$ such that ω_z is not a zero of $G(s)$ then, $\tilde{G}(s)$ can be written as $\tilde{G}(s) = (s^2+\omega_z^2)\sum_{i=1}^{N} \frac{\beta_i}{s^2+\omega_i^2}$.

Proof: At $s^2 = -w_z^2$, $\tilde{G}(s) = 0$. Substituting $s^2 = -w_z^2$ in $\tilde{G}(s)$ we have,

$$\tilde{G}(j\omega_z) = \sum_{i=1}^{N} \frac{\alpha_i}{-\omega_z^2+\omega_i^2} + D = 0$$

Thus, $D = -\sum_{i=1}^{N} \frac{\alpha_i}{-\omega_z^2+\omega_i^2}$

Substituting the value of D in $\tilde{G}(s)$ we get

$$\begin{aligned} \tilde{G}(s) &= \sum_{i=1}^{N} \frac{\alpha_i}{s^2+\omega_i^2} - \sum_{i=1}^{N} \frac{\alpha_i}{-\omega_z^2+\omega_i^2} \\ &= \sum_{i=1}^{N} \alpha_i \left(\frac{1}{s^2+\omega_i^2} - \frac{1}{\omega_i^2-\omega_z^2}\right) \end{aligned}$$

Let $\frac{1}{\omega_i^2-\omega_z^2} = a_i$. Then,

$$\begin{aligned} \tilde{G}(s) &= \sum_{i=1}^{N} \alpha_i \left(\frac{1 - a_i s^2 - a_i \omega_i^2}{s^2+\omega_i^2}\right) \\ &= \sum_{i=1}^{N} -\alpha_i a_i \left(\frac{s^2+\omega_i^2 - \frac{1}{a_i}}{s^2+\omega_i^2}\right) \end{aligned}$$

Note that $\omega_i^2 - \frac{1}{a_i} = \omega_z^2$. Thus,

$$\tilde{G}(s) = \sum_{i=1}^{N} -\alpha_i a_i \left(\frac{s^2+\omega_z^2}{s^2+\omega_i^2}\right)$$

Let $-\alpha_i a_i = \beta_i$. Then $\tilde{G}(s) = (s^2+\omega_z^2)\sum_{i=1}^{N} \frac{\beta_i}{s^2+\omega_i^2}$. ∎

This theorem shows that for a system obtained by adding N second order sections of the form $\frac{\alpha_i}{s^2+\omega_i^2}$, the addition of a feed-through term $D \in \mathbb{R}$ can effectively introduce a pair of complex conjugate (resonant) zeros. A typical pole-zero plot of the collocated transfer function before and after addition of the feed-through D term is shown in Figure 5. The pole location remains the same even after adding the feed-through term.

Using the *residue* function in MATLAB, the fixed structure form of the collocated transfer function of the piezoelectric laminate cantilever beam can be extracted from the identified model $G_{yu}(s)$ as shown in Figures 3 and 4. This is written as

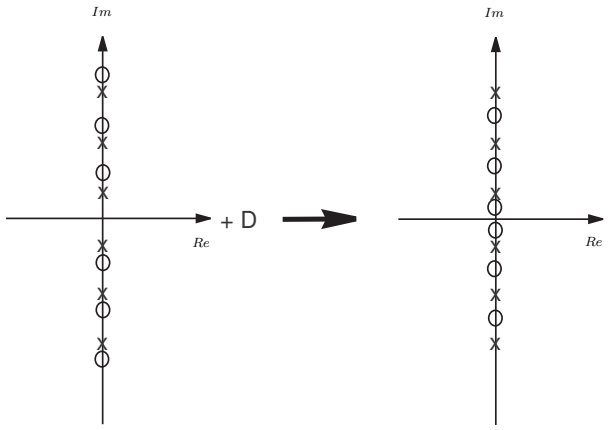

Fig. 5. Poles (x) and Zeros (o) of the collocated transfer function, before and after the addition of the feed-through term (D).

$$\begin{aligned} G_{yu}(s) &= \frac{225}{s^2+0.3854s+6035} + \frac{8971}{s^2+1.49s+217100} \\ &+ \frac{90960}{s^2+3.573s+1.697\times10^6} + 0.7456 \end{aligned}$$

Due to the fully parameterized nature of the identified model, the residuals of each second order section will also contain a small 's' term that can be neglected. Note that in this case, $G_{yu}(s) \equiv \tilde{G}(s)$ (defined in Theorem 2), where

$$G(s) = \frac{225}{s^2+0.3854s+6035} + \frac{8971}{s^2+1.49s+217100} + \frac{90960}{s^2+3.573s+1.697\times10^6}$$

and $D_1 = 0.7456$.

The first resonant mode of the cantilever beam is at a frequency of 12.33 Hz. By using Theorem 2, it is seen that a feed-through of $D_2 = -0.1372$ places a zero at 4.1858Hz (< 12.33 Hz). Combining D_1 and D_2, a feed-through term of $D_f = (-0.1372 - 0.7456) = -0.8828$, was added to $G_{yu}(s)$.

The addition of a low-frequency zero results in a phase inversion at DC relative to the original transfer function as explained in Theorem 2. The magnitude and phase response of the collocated open-loop and modified transfer functions, $G_{yu}(s)$ and $(G_{yu}(s)+D_f)$ respectively, are plotted in Figure 6. It is observed that the phase of the modified transfer function lies between 0 and -180 degrees; thus, a negative integral controller ($C(s) = \frac{-1}{s}$) in negative feedback, which adds a constant phase *lead* of 90 degrees will yield a loop transfer function whose phase response lies between +90 and -90 degrees, that is, the closed-loop system has a highly desirable phase margin of 90 degrees. The following section discusses the advantages and disadvantages of a simple integral controller, a lossy integral controller and a simple second-order band-pass filter type controller. The controller gain can be selected using the root-locus plot and

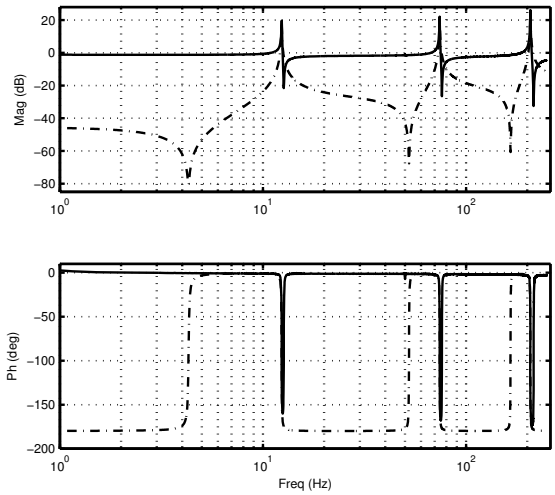

Fig. 6. collocated transfer function with (—) and without (- -) feed-through.

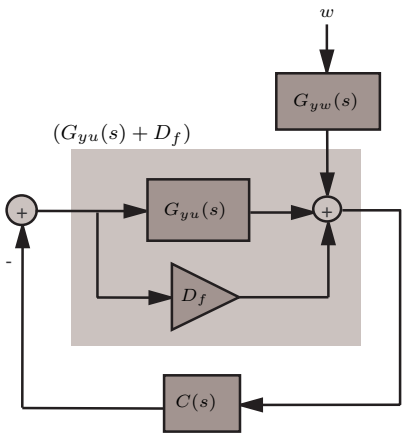

Fig. 7. Schematic diagram of the implemented IRC control strategy.

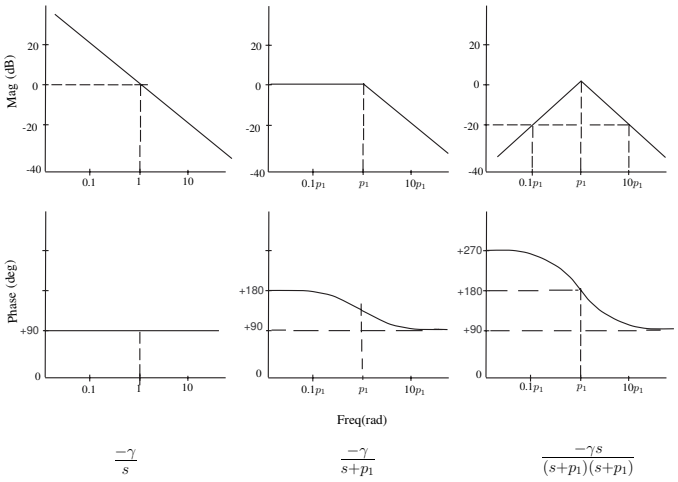

Fig. 8. Typical bode plots of the three possible controllers assuming $\gamma = 1$

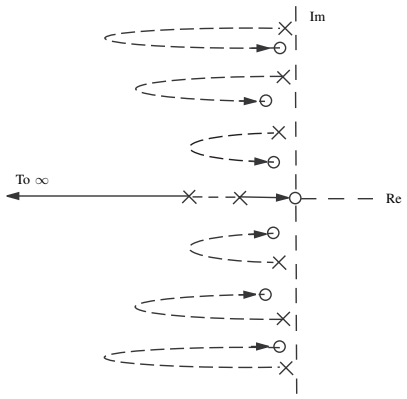

Fig. 9. Root-Locus plot showing the trajectories of the poles due to change in system gain.

can be targeted to damp specific modes. Subsection III-D will present a brief discussion on gain selection.

C. Controller design for zero-pole systems

As the following controller designs are motivated by the simple integrator, this control scheme is called the Integral Resonant Control, IRC. The block diagram of this proposed IRC scheme is shown in Figure 7. In the following discussion, three suitable controllers - direct integral control, its lossy variant and a simple band-pass filter type controller - are introduced and evaluated for performance and robustness. The frequency response of each controller is plotted in Figure 8.

- **Simple Integrator** $C(s) = \frac{-\gamma}{s}$: Integral control has been extensively researched and documented [15]. As it applies an unnecessarily high gain at low frequencies, it may lead to actuator saturation due to input amplification.
- **Lossy integrator** $C(s) = \frac{-\gamma}{s+p_1}$: This controller has reduced gain at low frequencies when compared to that applied by the pure integrator. It is necessary to select p_1 close to the first structural resonance frequency. The penalty associated with its implementation is of a slightly reduced closed-loop phase margin.
- **Band-pass filter** $C(s) = \frac{-\gamma s}{(s+p_1)(s+p_1)}$: To ensure the controller response rolls-off at low-frequencies, a controller with two poles at p_1 $rad.s^{-1}$ and a zero at 0 $rad.s^{-1}$ is suitable. The resulting closed-loop phase margin is inferior to that exhibited by the two previous controllers but the gain attenuation is greater. The phase margin can be further improved by implementing $C(s) = \frac{-\gamma s}{(s+p_1)(s+p_2)}$ where $p_2 < p_1$.

D. Gain selection

The gain of the IRC, γ, can be determined by analyzing the loop gain. A root-locus plot depicts the trajectories traveled by the poles with respect to increase in the system gain, see Figure 9. It is found that by increasing the controller gain, the poles follow a curve and finally reach the zeros they are paired with. This plot also reveals the damping of each pole along the trajectory. As the gain increases, the poles initially move away from the imaginary axis and the damping increases until it reaches a maximum point. Further increases in gain drag the pole closer to the imaginary axis and reduce the damping. Finally the pole is placed at the same position as its paired zero. At this position, the improvement in damping is negligible.

Thus, the gain of the controller can be chosen such that maximal damping performance is achieved at the in-band resonant modes that lie within the bandwidth of interest. To achieve maximum damping of higher frequency modes, higher gains are required. This high gain may place the low frequency poles close to the imaginary axis (with no significant increase in damping) and thus low frequency modes are not attenuated. As we are considering a cantilever beam with dominant low frequency dynamics (with the first resonant mode at 12.33 Hz), a gain that provides optimal damping of the first three structural modes is chosen. For the cantilever beam used in our experiments, the required gain was found to be $\gamma = 550$.

E. Summary

The IRC controller design process can be summarized in the following steps:

- **Step 1:** Measure the open-loop frequency response of the system and preferably obtain a model for the system as described in subsection III-A.
- **Step 2:** Use results in Subsection III-B. Determine the required feed-through term that adds a zero at a frequency lower than the first resonant mode of the system.
- **Step 3:** Design a controller of the form $C(s) = \frac{-\gamma s}{(s+p_1)(s+p_1)}$ by choosing p_1 to be approximately a decade lower in frequency than the first mode, see subsection III-C.
- **Step 4:** By plotting the root-locus, select a suitable gain which results in peak attenuation at resonant frequencies lying in the band of interest, see subsection III-D.
- **Step 5:** Implement IRC using either an analog or digital transfer function. Measure the open- and closed-loop frequency responses and check that they agree with the simulated results as shown in Section IV.

IV. Experimental results

The controller was digitally implemented using a dSPACE rapid prototyping system with a sampling frequency of 20 kHz. The continuous transfer function of the controller, given by $C(s) = \frac{-550s}{(s+0.3(2\pi))(s+0.3(2\pi))}$, was converted to a discrete transfer function using the zero order hold approximation. A time advance of one sample, achieved by multiplying the transfer function of the controller by the forward shift operator z, was incorporated into the control loop to account for the system delay. This is possible because $C(z)$ is strictly proper and has a relative degree of 1. Frequency responses are measured from the input disturbance w to the output tip displacement z of the cantilever beam, denoted by G_{zw}. Figure 10 (a) shows the simulated open- and closed-loop frequency responses while the measured open- and closed-loop frequency responses are shown in Figure 10 (b). The first three modes are attenuated by 22 dB, 24 dB and 21 dB respectively.

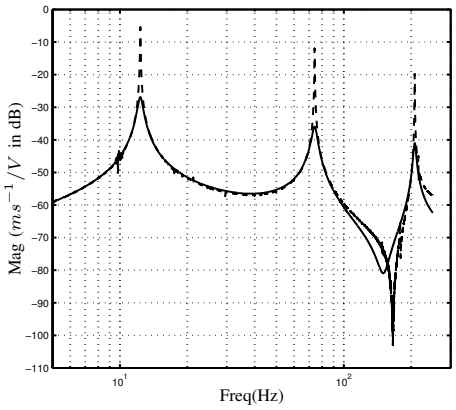

(a)

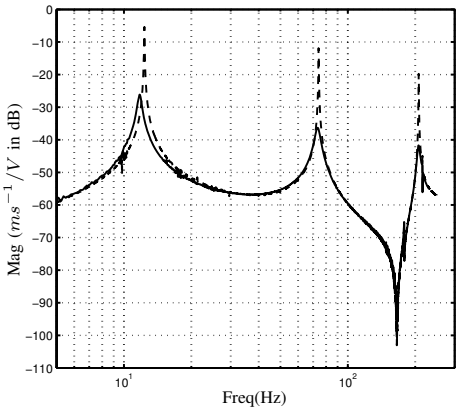

(b)

Fig. 10. Simulated (a) and experimental (b) open-loop (- -) and closed-loop (–) responses of the cantilever beam measured from disturbance input w to the tip displacement z.

Open- and closed-loop frequency responses are measured for a band of frequencies from 0 Hz to 2.5 kHz, to evaluate the controller performance, see Figure 11. This band captures the first eight resonant modes of the cantilever beam. Table I shows the attenuation achieved for the first eight modes.

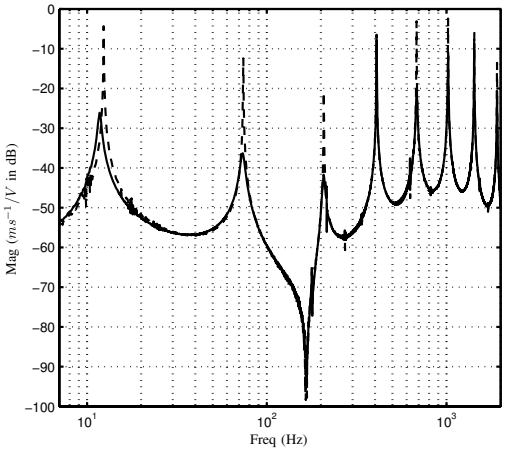

Fig. 11. Open- (- -) and closed-loop (—) system response for the first eight modes of the cantilever beam measured from disturbance input w to the tip displacement z.

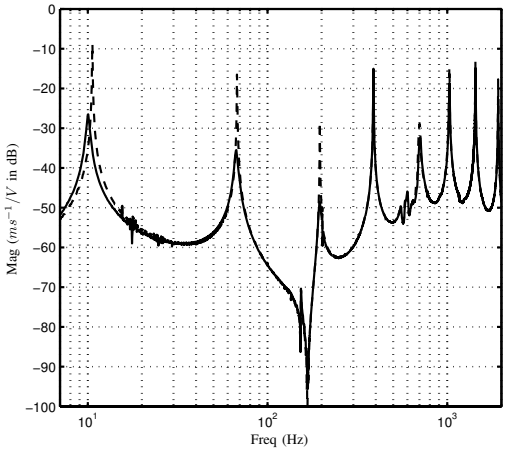

Fig. 12. Open- (- -) and closed-loop (—) system response for the additional mass-loaded cantilever beam measured from disturbance input w to the tip displacement z.

TABLE I

DAMPING FOR THE FIRST EIGHT MODES OF THE CANTILEVER BEAM

Mode Number	1	2	3	4	5	6	7	8
Frequency(Hz)	12.33	74.25	207.48	408.75	682.32	1020.85	1427.23	1914.01
Attenuation (dB)	22	24	21	0.7	16	9	3	7

TABLE II

DAMPING FOR THE FIRST EIGHT MODES FOR A CANTILEVER BEAM WITH ADDED MASS

Mode Number	1	2	3	4	5	6	7	8
Frequency(Hz)	10.625	67.48	195.76	356.68	702.38	1028.98	1435.82	1921.97
Attenuation(dB)	17	19	20	0.5	4	4	1	5

The minimal attenuation of the fourth mode is due to the position of the collocated patches.

Loading the beam with a mass introduces changes in the resonant mode frequencies. IRC's damping performance is evaluated for its robustness for variations in resonance frequencies by first loading the cantilever beam with a mass and then recording its open- and closed-loop responses. Loading the beam with a mass introduces changes in the resonant mode frequencies and is equivalent to adding uncertainty. It is seen that even though the additional mass shifts the resonant mode frequencies by as much as ten percent, there is minimal performance degradation. All of the eight modes show significant damping even with the mass present, see Figure 12. Table II documents the damping achieved on the loaded beam for the first eight modes.

V. CONCLUSIONS

A mathematical proof for the pole-zero interlacing found in the transfer functions of collocated smart structures is given. The effect of adding a feed-through to these transfer functions is the addition of a pair of resonant zeros at a particular frequency, depending on the magnitude and sign of the feed-through term. This effect is also mathematically formulated and a parametrized structure of the feed-through term in terms of frequencies at which it adds the resonant zeros is given. The phase response of the transfer functions of collocated smart structures show that by adding a pair of zeros at a frequency below the first resonant mode, simple first- or second-order controllers can provide good damping performance and stability margins. Three controllers motivated by the integral controller are proposed, and their performance benefits and drawbacks are discussed. The so-called Integral Resonant Control scheme, IRC, is implemented on a cantilever beam. This IRC scheme is shown to damp the first eight resonant modes of the cantilever beam by up to 24 dB even under resonance frequency uncertainties.

REFERENCES

[1] S. Salapaka, A. Sebastian, J. P. Clevland, and M. V. Salapaka, "Design identification and control of a fast nanopositioning device," in *Proc. American Control Conference*, May 2002, pp. 1966 – 1971.

[2] L. Vaillon and C. Philippe, "Passive and active microvibration control for very high pointing accuracy space systems." *Smart Materials and Structures*, vol. 8, no. 6, pp. 719–728, December 1999.

[3] S. Wu, T. L. Turner, and S. A. Rizzi, "Piezoelectric shunt vibration damping of an F-15 panel under high-acoustic excitation," in *Proc. SPIE Smart Structures and Materials: Damping and Isolation*, vol. 3989, 2000, pp. 276 – 287.

[4] E. F. Crawley and J. de Luis, "Use of piezoelectric actuators as elements of intelligent structures," *AIAA Journal*, vol. 25, no. 10, pp. 1373–1385, 1987.

[5] B. T. Wang and C. C. Wang, "Feasibility analysis of using piezoceramic transducers for cantilever beam modal testing," *Smart Materials and Structures*, vol. 6, no. 1, pp. 106–116, 1997.

[6] C. R. Fuller, S. J. Elliott, and P. A. Nelson, *Active Control of Vibration*. Academic Press, 1996.

[7] S. O. R. Moheimani and A. J. Fleming, *Piezoelectric transducers for vibration control and damping*. Springer-Verlag, 2006.

[8] I. R. Petersen and H. R. Pota, "Minimax LQG optimal control of a flexible beam," *Control Engineering Practice*, vol. 11, no. 11, pp. 1273–1287, November 2003.

[9] B. M. Chen, T. H. Lee, H. Chang-Chieh, Y. Guo, and S. Weerasooriya, "An H_∞ almost disturbance decoupling robust controller design for a piezoelectric bimorph actuator with hysteresis," *IEEE Transactions on Control Systems Technology*, vol. 7, no. 2, pp. 160–174, February 1999.

[10] J. L. Fanson and T. K. Caughey, "Positive position feedback-control for large space structures," *AIAA Journal*, vol. 28, no. 4, pp. 717–724, April 1990.
[11] C. W. de Silva, *Vibration Fundamentals and Practice*. CRC Press, 1999.
[12] H. R. Pota, S. O. R. Moheimani, and M. Smith., "Resonant controllers for smart structures," *Smart Materials and Structures*, vol. 11(1), no. 1, pp. 1 – 8, February 2002.
[13] T. McKelvey, H. Akcay, and L. Ljung, "Subspace based multivariable system identification from frequency response data," *IEEE Transactions on Automatic Control*, vol. 41, no. 7, pp. 960–978, July 1996.
[14] G. D. Martin, "On the control of flexible mechanical systems," Ph.D. dissertation, Stanford University, U.S.A., 1978.
[15] A. Preumont, *Vibration Control of Active Structures: An Introduction*. Kluwer, 1997.
[16] P. C. Hughes, "Space structure vibration modes: how many exist? which ones are important?" *IEEE Control Systems Magazine*, vol. 8, no. 1, pp. 22–28, February 1987.
[17] R. L. Clark, "Accounting for out-of-bandwidth modes in the assumed modes approach: implications on collocated output feedback control," *Transactions ASME Journal of Dynamic Systems Measurement and Control*, vol. 119, pp. 390–395, 1997.